Volume 15, Issue 2, 152513 (1-14)

Iranian Journal of Catalysis (IJC)

https://doi.org/10.57647/j.ijc.2025.1502.13

Novel approaches for electrocatalytic CO_2 reduction into higher hydrocarbons

Tayyab Ashfaq Butt*

Department of Civil Engineering, College of Engineering, University of Hail, Ha'il, Saudi Arabia.

***Corresponding author:** ta.butt@uoh.edu.sa

Review Paper

Received:
8 February 2025
Revised:
30 March 2025
Accepted:
26 April 2025
Published online:
3 May 2025

Abstract:

Creative solutions are required to overcome global warming due to the rising CO_2 emissions from the utilization of fossil fuels. Through the conversion of CO_2 into useful chemicals and alternative fuels, CO_2 capture and utilization (CCU) technologies present a possible avenue for action. This article critically investigates current developments in electrocatalytic CO_2 reduction and emphasizes the use of C-C coupling processes to produce higher hydrocarbons. The research investigates the difficulties related to catalyst stability, product selectivity, and energy efficiency while examining benchmark studies on CO_2 electroreduction into C_1 and C_2 products. Noteworthy advancements in the electrochemical Fischer-Tropsch (FT) method and molecular catalysts for the synthesis of longer-chain hydrocarbons are discussed in detail. The review also covers recent advances in catalyst design, including the creation of proton exchange membrane systems with long-term stability and the highest CO_2 conversion efficiencies under reaction conditions relevant to the industry. Optimizing catalyst design and surface modifications to improve performance and overcome competitive side reactions, such as the hydrogen evolution reaction (HER), are potential future research paths. These developments could help the world's attempts to achieve carbon neutrality by opening the door for scalable and sustainable CO_2 conversion methods.

Keywords: CO_2 reduction; Electrochemical Fischer-Tropsch reaction; Higher hydrocarbons; Molecular catalyst; Reaction mechanism

1. Introduction

Fossil fuel consumption and human activities, including land use and deforestation, have increased CO_2 emissions to approximately 37 Gt per year in 2022 [1]. Several decarbonization initiatives are being investigated to meet this challenging environmental goal [2]. One way to convert CO_2 emissions into useful carbon-based compounds and fuels is through carbon capture and utilization (CCU) [3, 4]. In CCU plans, CO_2 emissions are collected from large carbon-emitting sources (such as the production of steel and cement) [5] or directly from the environment through the use of direct air capture (DAC) technology [6]. The carbon-based compounds that are created from this CO_2 can be easily integrated into current supply chains and industrial processes. A viable path to closing the carbon cycle is through CCU [7] as illustrated in figure 1. The production of fuels and chemicals depends heavily on fossil fuels, amounting to approximately 2.5 gigatons of CO_2 emissions annually (chemical synthesis, red process) [2]. One alternate method for producing these compounds sustainably is CO_2 electroreduction reaction (CO_2RR), which uses water, renewable energy, and CO_2 extracted from flue gas or the atmosphere at ambient temperatures. Increasing CO_2RR to handle gigatons of CO_2 emissions presents significant resource requirements, as well as performance and lifespan issues with CO_2RR systems [1]. To establish a seamless transition between CO_2 capture technologies and catalyst development, it is essential to highlight the interdependence of these processes. While efficient CO_2 capture methods enable the capturing of carbon dioxide from industrial emissions, their true impact lies in the ability to convert captured CO_2 into different useful products. This conversion relies on the discovery of highly selective and stable electrocatalysts that can efficiently drive CO_2 reduction reactions under practical conditions. However, conventional CO_2 capture methods often produce CO_2 in a form that requires further purification and compression, adding to energy costs. Advanced catalytic systems must therefore be designed not only to enhance product selectivity but also to integrate effectively with CO_2 capture processes, minimizing addi-

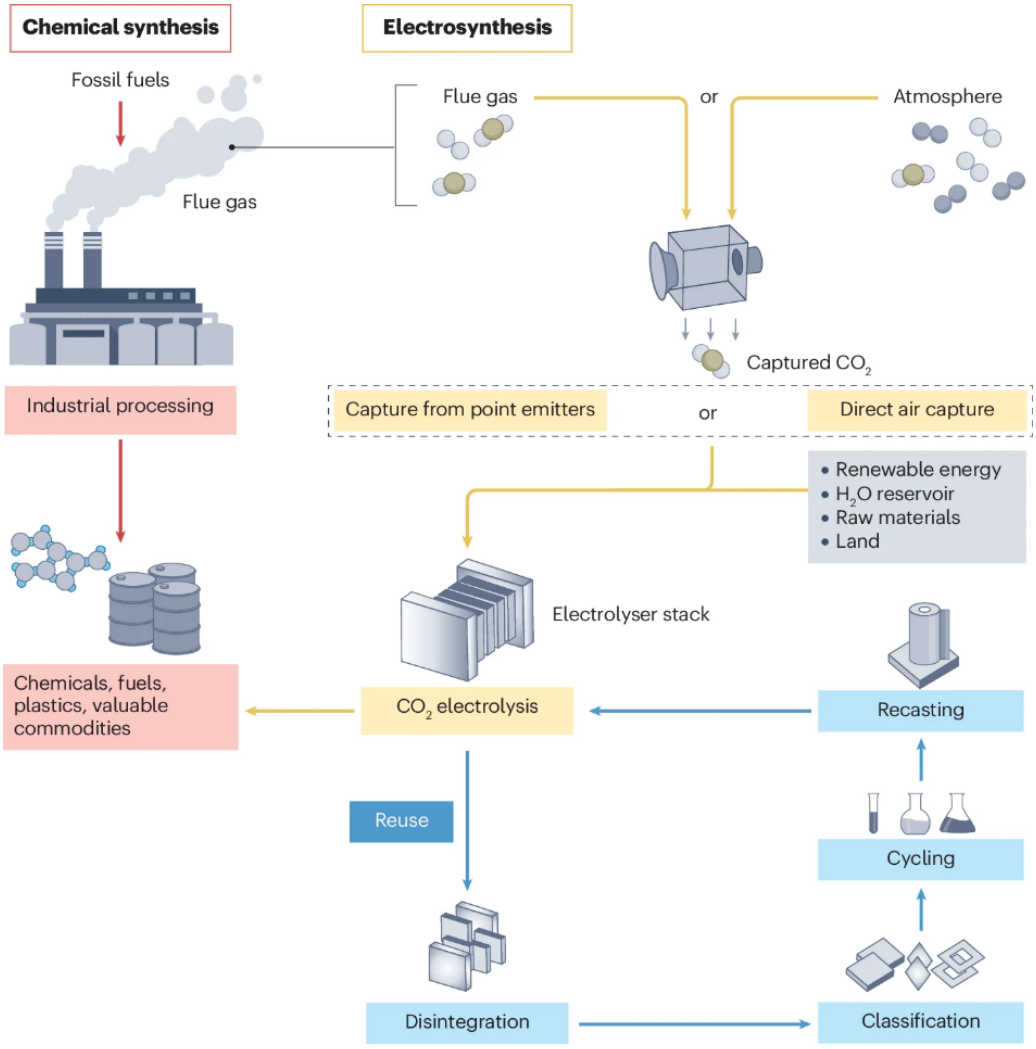

Figure 1. CO_2 RR alternative to conventional fuels and chemicals synthesis [1] Copyright Nature 2024.

tional energy inputs. By bridging these aspects, the transition from CO_2 capture to electrochemical conversion can be optimized to create a more sustainable and economically viable carbon utilization framework.

Along with the immediate replacement of fossil fuels with alternative renewable energy resources, there is also an urgent need to convert the emitted CO_2 into commercial chemicals (as presented in figure 2) to reduce the overall carbon footprint in the environment [9–11]. CO_2 conversion into different chemicals has many challenges [12] such as CO_2 capturing and storage, hydrogen production and storage, chemical reaction setup, design of a suitable catalyst, and engineering parameters to optimize the reaction conditions [13, 14]. As far as hydrogen availability is concerned, the electrochemical CO_2 reduction process doesn't need additional hydrogen, unlike thermochemical CO_2 hydrogenation processes [15–24]. Furthermore, the electrochemical processes are more versatile and sustainable because their renewable and less polluting, causing nature [25–27]. Here in this article few benchmark studies related to CO_2 capturing technologies, CO_2 electrochemical reduction into C_1 compounds at high faradic efficiency and current density with long-term time activity, CO_2 reduction into C_{2+} products with the explanation of C-C coupling mechanism over the molecular catalyst and electrochemical Fischer Tropsch CO_2 reduction into high hydrocarbons have been critically analyzed and presented in a simple way to make them easy to understand for the broader category of researcher and related persons. Previously, a review explored CO_2RR as an integrating carbon capture with electrochemical transformation to enhance efficiency, reduce energy consumption, and enable sustainable carbon recycling [45, 46]. Another article highlights advancements in electrocatalytic CO_2 and CO reduction, focusing on catalyst development, reactor engineering, mechanistic insights, and commercial viability to accelerate the deployment of CO_2 electrolysis for sustainable chemical manufacturing [47]. R. Sharifian's review examines recent advances in electrochemical CO_2 capture via pH-swing processes, analyzing energy efficiency, system parameters, and the potential for integrating CO_2 conversion into a sustainable electrified carbon economy [48]. A summary of the different processes for CO_2 capturing and conversion has been given in Table 1.

A recent study published in Nature [49] demonstrates that an electrochemical charged carbon electrode can effectively capture CO_2 from the environment, and regenerate at lower temperatures of 100 °C as compared to the conventional method of alkalized solution-based CO_2 capturing, which

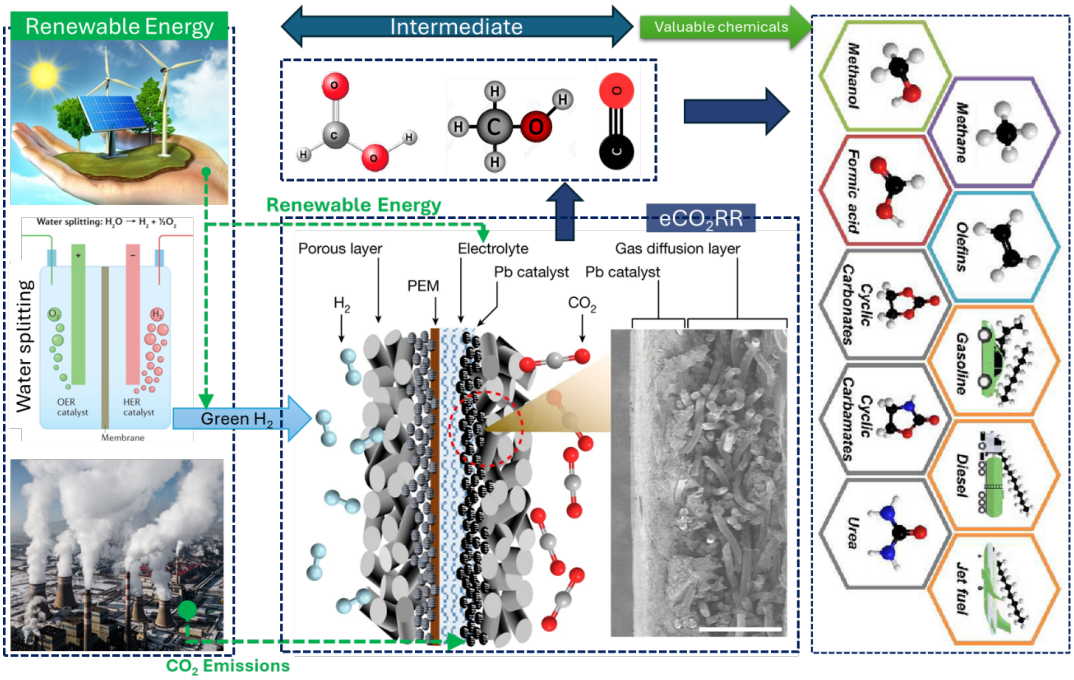

Figure 2. Process flow diagram for renewable energy-based CO_2 reduction and subsequent transformation into alternative commercial chemicals [8] Copyright Nature 2024.

requires higher temperatures for regeneration [50]. To guarantee that captured CO_2 is securely deposited in geological rock formations, storage capacity must be high, and continuous monitoring must be conducted. Coupling CO_2 capturing with conversion may be the sustainable approach to achieving net carbon neutrality in the next half-century. Electrochemical CO_2 reduction received much attention because of its environmental friendliness [51]. It can be operated with electricity produced from solar and wind, in addition to no additional hydrogen requirement [52]. Significant progress has been made in catalyst development and reactor design, but challenges remain in enhancing product selectivity, improving system stability, and scaling up for industrial applications. This review provides a comprehensive overview of current progress in CO_2RR, focusing on catalyst innovations, mechanistic insights, and emerging electrochemical strategies for higher hydrocarbon synthesis. Additionally, I discussed the integration of CO_2 capture with electrochemical conversion, emphasizing strategies to improve energy efficiency and process feasibility. By addressing key challenges and potential solutions, this review aims to provide a roadmap for advancing CO_2RR technologies toward practical and sustainable applications.

Table 1. Comparison of CO_2 capture, CO_2 reduction, and combined CO_2 capture and conversion technologies.

Aspect	Electrochemical CO_2 Capture Technologies	Advances in CO_2 Electroreduction	Electrochemical Conversion of Captured CO_2
Main Focus	Electrochemical CO_2 capture via pH-swing processes	Catalyst development, reactor design, and mechanistic insights for CO_2 electroreduction	Integration of CO_2 capture and electrochemical conversion
Key Approach	pH-swing methods (electrolysis, electrodialysis, redox, capacitive deionization)	Selective electrocatalysts, reaction mechanisms, and commercial prospects	Electrochemically reactive CO_2 capture
Challenges Addressed	Cost, energy efficiency, and material availability	Enhancing selectivity, scalability, and commercial viability of CO_2 electrolysis	Reducing energy-intensive steps in CO_2 capture and conversion
Technological Advances	Improved efficiency of pH-swing methods and integration with renewable energy	Nanoporous Ag, Cu-based bimetallic catalysts, in situ spectroscopy, techno-economic analysis	Capture media integration, catalyst selection, and reactor optimization.
Commercial Potential	Potential for a circular carbon economy with renewable electricity	Highlights barriers to commercialization and proposes solutions	Offers a more efficient alternative to traditional CO_2 capture and conversion
Future Directions	Reducing costs, improving electrode/membrane materials, and enhancing conversion efficiency	Overcoming pollutant effects, improving process modeling, and accelerating industrial adoption	Optimizing integrated systems for large-scale deployment

Challenges in CO_2RR

CO_2RR faces several challenges that hinder its widespread implementation for sustainable chemical production. One of the primary obstacles is the low selectivity and efficiency of catalysts, as CO_2 reduction is often challenged by the hydrogen evolution reaction (HER), leading to reduced faradaic efficiency [53]. Additionally, most catalysts suffer from stability issues, undergoing deactivation due to surface restructuring, metal leaching, or carbonate formation. Another significant challenge is mass transport limitations, especially in aqueous systems where CO_2 solubility is low, restricting the reaction rate. A brief summary of the performance of different catalysts under different reaction conditions has been given in Table 2. Moreover, CO_2RR requires precise control over reaction pathways to achieve selective production of valuable multi-carbon products, which is influenced by catalyst composition, surface morphology, and electrolyte conditions. Lastly, the scalability and economic feasibility of CO_2RR remain concerns, as current electrolyzer designs require high overpotentials and costly materials, limiting industrial deployment. To overcome these challenges, there is a dire need for catalyst engineering, reactor design, electrolyte optimization, and integration with renewable energy sources to make CO_2RR a viable solution for carbon-neutral chemical synthesis.

Most catalysts exhibit excellent performance in basic solutions, where precipitation from carbonate production deactivates the catalyst. As a benchmark, Fang et al. [9] recently published their work in Nature, which demonstrated a high single-pass efficiency of 91% for CO_2 conversion, with a current density (CD) of 600 mA, HCOOH faradic efficiency of 93%, and high stability for more than 5200 h in acidic conditions, making it suitable for commercialization. However, the synthesis of higher hydrocarbons is still a challenging task for researchers. Recently few studies have been published that showed the synthesis of C_3 products but with a very selectivity of around 12% of propanol [54], for commercial-scale applications catalyst stability and product selectivity are highly important, and because of that some novel approaches such as the application of molecular catalysts, low-temperature CO_2 electroreduction, electrochemical Fischer Tropsch CO_2 reduction are important to consider for its commercialization.

Highly durable catalyst for CO_2 reduction

The use of acid electrolytes to reduce the carbonate formation was the main motivation of the study reported by Wensheng Fang and his co-workers [9], where a CO_2 reduction reaction coupled with an H^+ oxidation reaction to produce formic acid (HCOOH) and carbonate formation could be avoided. The major achievement is developing a system with a membrane that can exchange protons and that can convert CO_2 into HCOOH over a catalyst prepared from the battery waste, usually consisting of lead acid. This system demonstrates the highest single pass CO_2 conversion efficiency of 91% at a CD of 600 mA cm^{-2} and an approximate cell voltage of 2.2 V, and shows the stability for more than 5200 h, which produced formic acid with a

Table 2. Electrochemical performance of recent Cu-based catalysts for C_{2+} products, highlighting their respective Faradaic efficiency (FE), current density (CD), and applied potential across various electrolyte concentrations and reactor configurations.

Catalyst	Electrolyte	Potential (Vs RHE)	CD (mA/cm^2)	Partial CD (mA/cm^2)	FE C_{2+}	Reactor type	References
Cu-Pd bimetallic	1 M KCl	-1.15	200	225	75.6	Flow cell	[28]
Cu/Cu_2O	1 M KOH	-1.06	25	–	58	H cell	[29]
Cu_2O@CuBTC	0.1 M $KHCO_3$	-1.05	–	256	64.2	flow cell	[30]
CuO-ZrO_2		-1.50	–	200	82.3	flow cell	[31]
Cu_2O-Cu NCs	1 M KOH	-1.00	500	–	77.4	flow cell	[32]
Cu@Cu_2O		-1.08	15	–	79	H cell	[33]
CuxAly-OD	1 M KOH	-1.68	693	565	81.6	flow cell	[34]
Cu@Salen-PIL	1 M KOH	-0.80	–	263	80.9	flow cell	[35]
2.7% CuOx -R	3 M KOH	-0.90	289	245	84.7	flow cell	[36]
$Cu100Zn_{4.9}$	0.1 M CsI	-1.28	40	–	75	H cell	[37]
CuZn	1 M KOH	-1.17	140	–	80	H cell	[35]
Cu cavities	1 M KOH	-0.59	186	605	75.6	flow cell	[38]
Cu_9Zn1	2 M KOH	-1.15	400	–	88.5	flow cell	[39]
Cu_2O@C/N	0.1 M $KHCO_3$	-0.90	–	245	75.9	flow cell	[40]
B-CuO	0.5 M $KHCO_3$	-1.00	30	–	55.7	flow cell	[36]
Cu_2O/Cu	1 M KOH	-1.10	1003	–	80.4	flow cell	[41]
Cu_2O-xSe/Cu/NC	1 M KOH	-1.40	30.44	–	71.6	H cell	[42]
Cu@C	0.1 M CsI	-1.20	–	323	80.5	flow cell	[43]
CuNPs	1 M $KHCO_3$	-3.80	–	356	71.1	flow cell	[44]

faradic efficiency over 93%.

Reaction mechanism for HCOOH production

By combining experimental observation and Density Functional Theory (DFT) calculation (as presented in figure 3), the CO_2RR starts with the chemical absorption of CO_2 on the interface of Pb-$PbCO_3$. The CO_2 bond angle and Pb electronic state were considered to investigate the extent of the chemical activation and electroreduction process. The interface between Pb and $PbCO_3$ showed the lowest Gibbs free energy for the CO_2RR to HCOOH. This is due to the strong adsorption of CO_2 and the formation of a carbonate, indicating a high activity level for the theoretical CO_2 reduction reaction as presented in figure 3 (b). CO_2 adsorption was the priority on the Pb-$PbCO_3$ compared with H* adsorption because of the favorable CO_2 adsorption energy (−0.62 eV). The competitive HER reaction (which can occur at 0.50 eV) was suppressed because of the lower hydrogenation energy of CO_2 to HCOOH, about 0.31 and 0.48 eV on the Pb-$PbCO_3$ interface. The lower energy shift of CO_2RR is responsible for the higher activity of HCOOH formation and suppression of HER. Even at a lower potential of around 1.0 V, CO_2 adsorption is still more favorable as compared to H* adsorption on the interface of Pb-$PbCO_3$, as illustrated in figure 3 (c). The electrochemical CO_2RR stages exhibited a reduced energy change compared to HER, indicating that CO_2RR is the predominant reaction compared to HER. This allows CO_2RR to function in acidic electrolytes without carbonate formation.

This work gives new insight into CO_2RR under industrial-relevant conditions without the use of alkaline conditions, which cause rapid deactivation of the catalyst by carbonate formation. This work would provide a baseline for the design of a new catalytic system with the best activity and long-term stability over several months. The key concept for new research in this area would be the catalyst design and surface modification to overcome the HER reaction, which is a main competitive reaction in CO_2 reduction, hindering the commercialization of the process. The current direction is the design of effective catalysts with the same activity and durability for the synthesis of other important chemicals such as CH_4, CH_3OH, C_2H_5OH, and C_3H_7OH, as already reported by other researchers [54], but selectivity and catalytic activity are not so high. During electrochemical reduction of CO_2, C-C coupling is a major challenge to produce commercial chemicals such as C_2=C_4 olefines and C_{2+} alcohols or hydrocarbons.

Molecular catalysts for higher hydrocarbon synthesis

Metallic catalysts have been widely used for the CO_2 reduction reaction, including single-atom catalysts, nanoparticles, dual-atom catalysts, and bimetallic catalysts. Recently some studies have reported that the use of molecular catalysts can assist the C-C coupling during CO_2RR by providing two active sites for the adsorption of CO_2 and performing reductions and C-C coupling reaction [54], unlike the metallic catalysts which usually have comparatively higher distance between two active sites [20, 55], creating hinderance between C-C coupling reactions [56–58]. The second reason could be the comparative suppression of HER reaction over the molecular catalyst [57, 59–61] as compared to metallic catalysts, which are more active towards a competitive reaction such as HER during CO_2RR [56].

In a study published by Sakamoto et al., the catalytic performance of Cu-based molecular catalysts in CO_2 electroreduction was extensively examined across varied potentials and

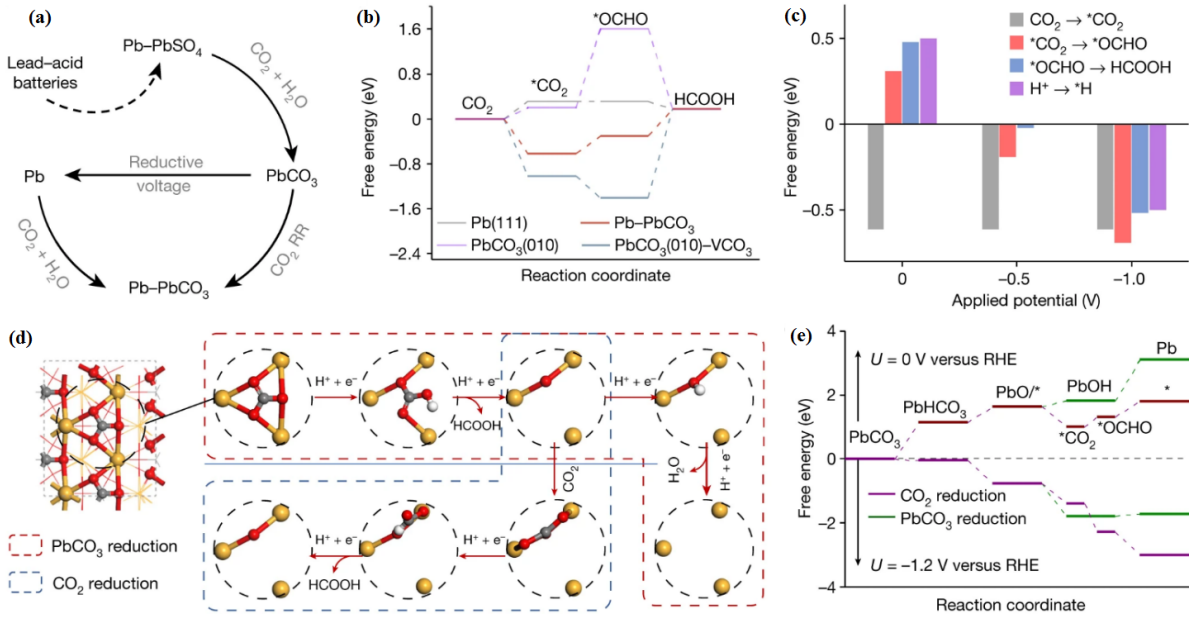

Figure 3. (a) Diagram illustrating the phase transition of the r-Pb catalyst. (b) Free energy profile for CO_2 reduction on active Pb sites, where $PbCO_3$(010)-VCO_3 signifies a carbonate vacancy in $PbCO_3$(010). (c) Variation in free energy during reactions under different applied potentials. (d) Conceptual representation of the catalytic mechanism driven by solid-state transformation. White, grey, red, and orange spheres correspond to H, C, O, and Pb atoms, respectively. (e) Free energy profile showing the reduction of $PbCO_3$ and CO_2 during the phase transition. The asterisk (*) marks the PbO configuration, which acts as the active site for CO_2 reduction, while U denotes the applied potential used in DFT simulations. Reprinted with permission from [9] Copyright Nature 2024.

catalyst compositions. Faradaic efficiency (FE) was measured throughout a potential range of −2.2 V to −1.4 V vs. Ag/AgCl for a variety of CO_2 reduction products, such as methane (CH_4), ethylene (C_2H_4), ethanol (C_2H_5OH), carbon monoxide (CO), and formic acid (HCOOH), as shown in figure 4 (a). The efficiency for C_2H_4 and C_2H_5OH improves while the FE for CH_4 drops with reduced negative potentials. A significant shift in the product distribution towards more carbon-containing products is observed as the potential becomes less negative. Furthermore, the creation of hydrogen (H_2) is found at all potentials, and its efficiency decreases at less negative potentials, demonstrating that proton reduction and CO_2 reduction are competitive processes [54].

Figure 4 (b) illustrates how the performance of several Cu-based catalysts is compared. It shows that the CuBr-4PP catalyst outperforms CuBr-BisM and CuBr-12B, which demonstrate much lower efficiencies for C_3 product formation, in terms of FE for 1-propanol (C_3H_7OH) synthesis. CuBr-4PP also performs exceptionally well in the synthesis of C_2 products, especially ethanol (C_2H_5OH), as shown in figure 4 (c), suggesting that it has improved multi-carbon product synthesis capabilities. On the other hand, the other catalysts show very low efficiency for these products, highlighting CuBr-4PP's special catalytic qualities. A more thorough examination of the C_1 product efficiencies in figure 4 (d) demonstrates that CuBr-4PP is versatile in catalyzing a variety of reaction pathways, as evidenced by the wide spectrum of C_1 products (CO, CH_4, HCOOH, and H_2) that it enables the formation of. On the other hand, CuBr-12B and CuBr-BisM exhibit more selective behavior, with CuBr-12B showing a preference for $*CH_3$ generation in particular [54].

Figure 4 (e) illustrates the hypothesized reaction process, which sheds light on the catalytic pathways of CuBr-4PP. According to the schematic, CO_2 is first adsorbed and then goes through a series of reduction and protonation processes that create intermediates (C_1, C_2, and C_3) before producing the final products. The strategy demonstrates that the CuBr-4PP stabilizes important intermediates, making it easier and more efficient to produce higher carbon products like C_2H_5OH and C_3H_7OH. CuBr-4PP could be a better option for further development in sustainable fuel and chemical production because of its exceptional catalytic performance in CO_2 electroreduction, especially in boosting the creation of multi-carbon products, as demonstrated by this thorough analysis.

A schematic diagram of the apparatus used to obtain Surface-Enhanced Raman Scattering (SERS) signals may be shown in figure 5 (a). An incoming 532 nm laser beam is used in the setup to target a layer of plasmonic and molecular nanoparticles on carbon paper. For basic understanding of the chemical intermediates during CO_2 reduction, this arrangement is essential.

The SERS spectra of the CuBr-4PP catalyst in CO_2 are displayed in figure 5 (b) at two different applied potentials (−1.2 V and −1.8 V) as well as without any potential applied. Diverse peaks in the spectra are indicative of various Cu-CO compounds. Notably, the $[Cu\text{-}CO\text{-}Cu]^+$, $[Cu\text{-}CHO\text{-}Cu]^+$, and $[Cu\text{-}CHOCO\text{-}Cu]^0$ intermediates correspond to the peaks at 2100 cm^{-1}, 1970 cm^{-1}, and 1850 cm^{-1}, respectively. This emergence and shifting in response to peaks with respect to the applied potential show the trends for forming and changing intermediates during the catalytic process.

SERS spectra at various potentials (−0.8 V, −1.2 V, −1.6 V, and −2.0 V) are shown in figure 5 (c), with an emphasis on the lower wavenumber region. The peaks located approximately at 1550 cm^{-1} are attributed to different intermediates of CO_2 reduction, including $[Cu\text{-}CHOCO\text{-}Cu]^0$ and $[Cu\text{-}CHOCHOCHO\text{-}Cu]^0$. The progressive reduction process and the transformation of intermediates into end products are suggested by the gradual decrease in peak intensity with rising negative potential.

Lastly, a thorough mechanistic pathway for CO_2 reduction on the dinuclear Cu(I) catalyst is shown in figure 5 (d), which also highlights the CO stretching frequencies (νCO) and related energy barriers (ΔG). The $[Cu\text{-}Br, CO\text{-}Cu]^0$ in-

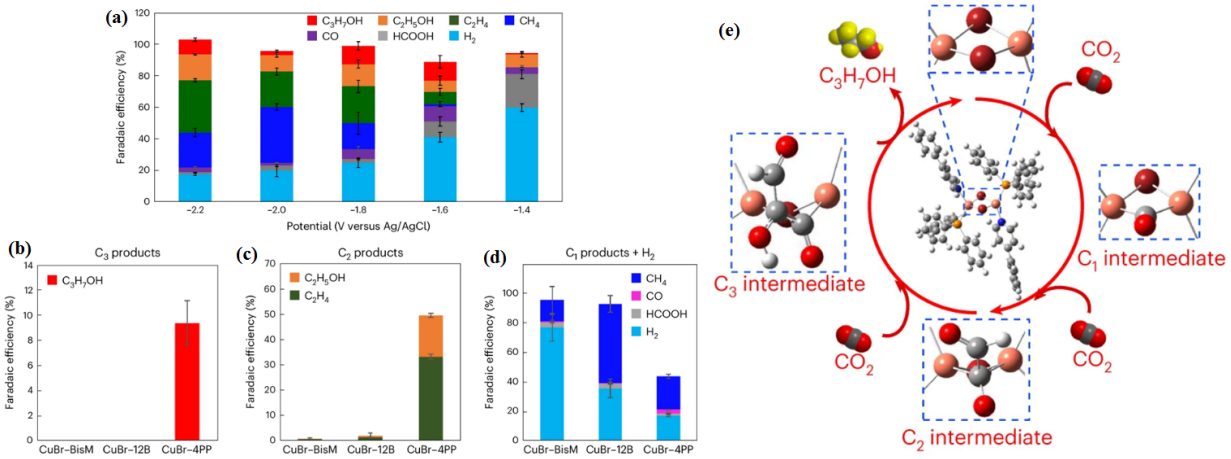

Figure 4. (a), After one hour of CO_2 reduction, the faradaic efficiency of different reduction products was evaluated using CuBr-4PP electrodes in a 0.5 M $KHCO_3$ electrolyte. When employing CuBr-BisM, CuBr-12B, and CuBr-4PP electrodes under identical conditions, various reduction products were detected at −2.2 V vs Ag/AgCl, including C_3 compounds (b), C_2 compounds (c), and a combination of C_1 products and H_2 (d). The error bars represent the standard error from three independent measurements. (d) An image illustrating the formation of C_3H_7OH through CO_2 reduction using a molecular catalyst [54] Copyright Nature 2024.

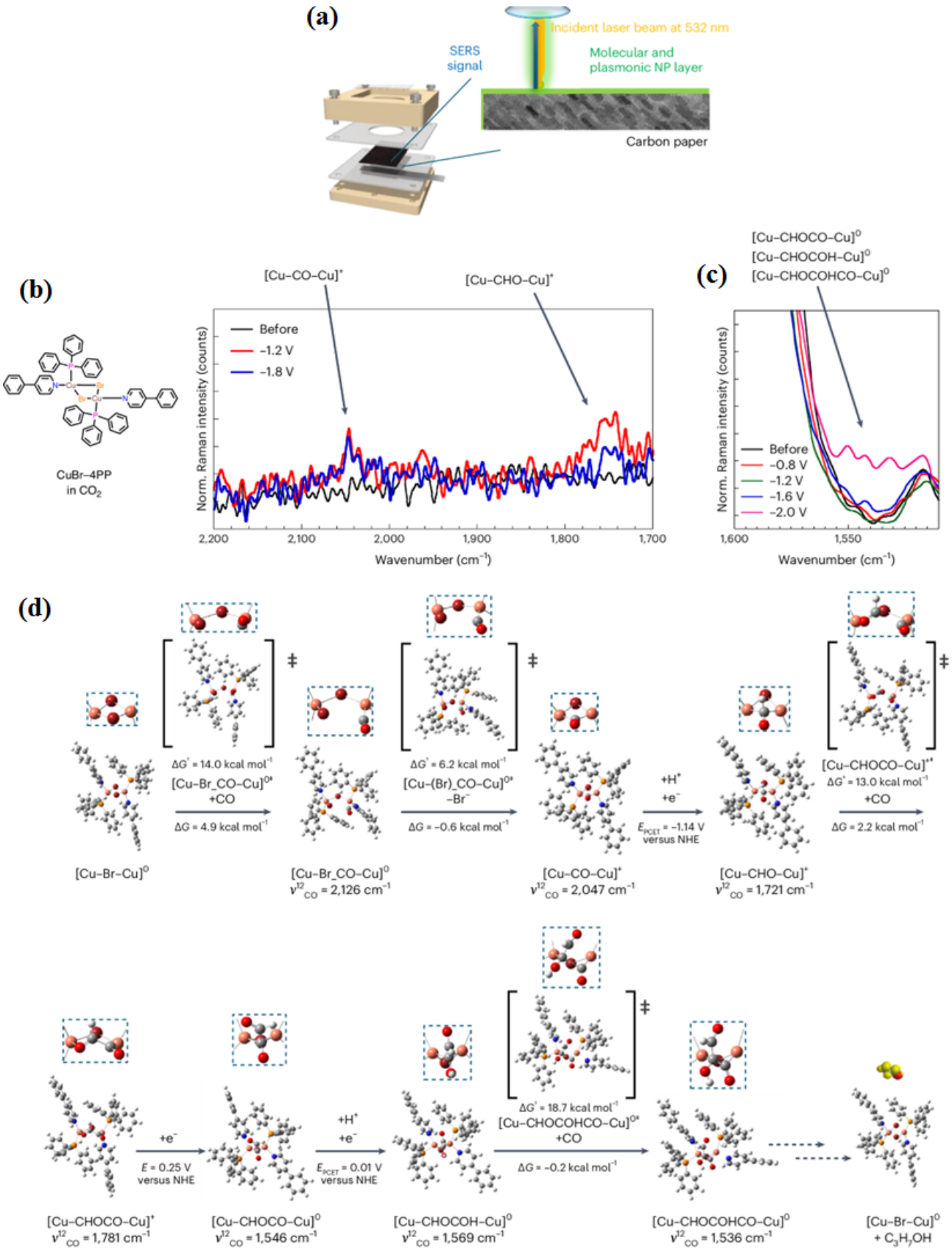

Figure 5. (a) Schematic of the molecular operando SERS measurement system. (b, c) Operando SERS spectra of CuBr-4PP under CO_2, recorded in the 1,700−2,200 cm^{-1} (b) and 1,510−1,600 cm^{-1} (c) regions. (d) Computed CORR electrocatalytic reaction pathway for CuBr-4PP, following a protonation-electron coupling mechanism. The calculated free-energy changes (ΔG) and reduction potentials (E) are presented in kcal/mol and volts versus NHE, respectively. The dashed frames highlight magnified views of the regions surrounding the Cu centers [54] Copyright Nature 2024.

termediate (νCO) = 2126 cm^{-1} is formed at the start of the catalytic cycle. It then goes through many proton and electron transfers, which finally result in the creation of the $[Cu\text{-}CHOCO\text{-}Cu]^0$ and $[Cu\text{-}CHOCHOCHO\text{-}Cu]^0$ intermediates. Following their conversion to the final product, these species produce C_2H_5OH along with other byproducts.

Electrochemical FT-CO_2 reduction reaction

The development of substitute catalysts that can produce a product with multi-carbon, has not shown much progress. It is noteworthy that many catalysts exhibiting measurable activity share nickel as a common element. For example, Ni-Ga alloys have achieved Faradaic efficiencies below 2% for ethylene and ethane, while nickel phosphides have demonstrated selectivity for CO_2 reduction, producing a C_3 and a C_4 oxy-hydrocarbon-methylglyoxal and 2,3-furandiol, respectively-at extremely low current densities and minimal overpotentials of just 10 mV. [62]. Previous studies on metallic nickel with a 60 atm CO_2 feed have reported the formation of hydrocarbons containing up to four carbon atoms, though with relatively low yields (1%). Interestingly, these Ni-based systems appear to promote C-C coupling, despite earlier findings by Hori et al., which indicated that metallic nickel is highly susceptible to CO contamination during CO_2 reduction. This contamination could account for its strong tendency toward the parasitic hydrogen evolution reaction [24, 63, 64].

Recent studies have revealed that inorganic nickel oxygenates (INOs), such as nickel phosphate, exhibit unexpectedly high activity for CO_2 reduction. These catalysts can achieve total Faradaic efficiencies of up to 30% for carbon-based products. Notably, they demonstrate remarkable selectivity (FE $\approx$ 16%) for hydrocarbon formation, with C_{3+} hydrocarbons being particularly prominent [65–67]. As shown in figure 6, Faradaic efficiencies of 6.5% have been achieved for C_3-C_6 hydrocarbon products, with partial current densities of j = 0.91 mA/cm^2. This performance surpasses that of the most advanced copper-based catalysts, which exhibit a Faradaic efficiency of 2.9% and j = 0.22 mA/cm^2 for C_3 and C_4 hydrocarbons, as well as any other reported materials [19, 22].

It has been determined that $Ni^{\delta+}$ catalytic sites linked to Ni-O bonds exist and are stable during the CO_2RR by combining theoretical and experimental methods, such as operando spectroscopy [62]. $Ni^{\delta+}$ sites bind CO modestly, preventing poisoning, in contrast to Ni^0. The reduction of various C_1 molecules, including formaldehyde, formic acid, and CO, has led to the identification of reactive intermediates believed to play a key role in a Fischer-Tropsch-like insertion mechanism for initiating and extending hydrocarbon chains [62]. It has been found that the polarization of Ni sites is essential for tuning the adsorption strength of key reaction

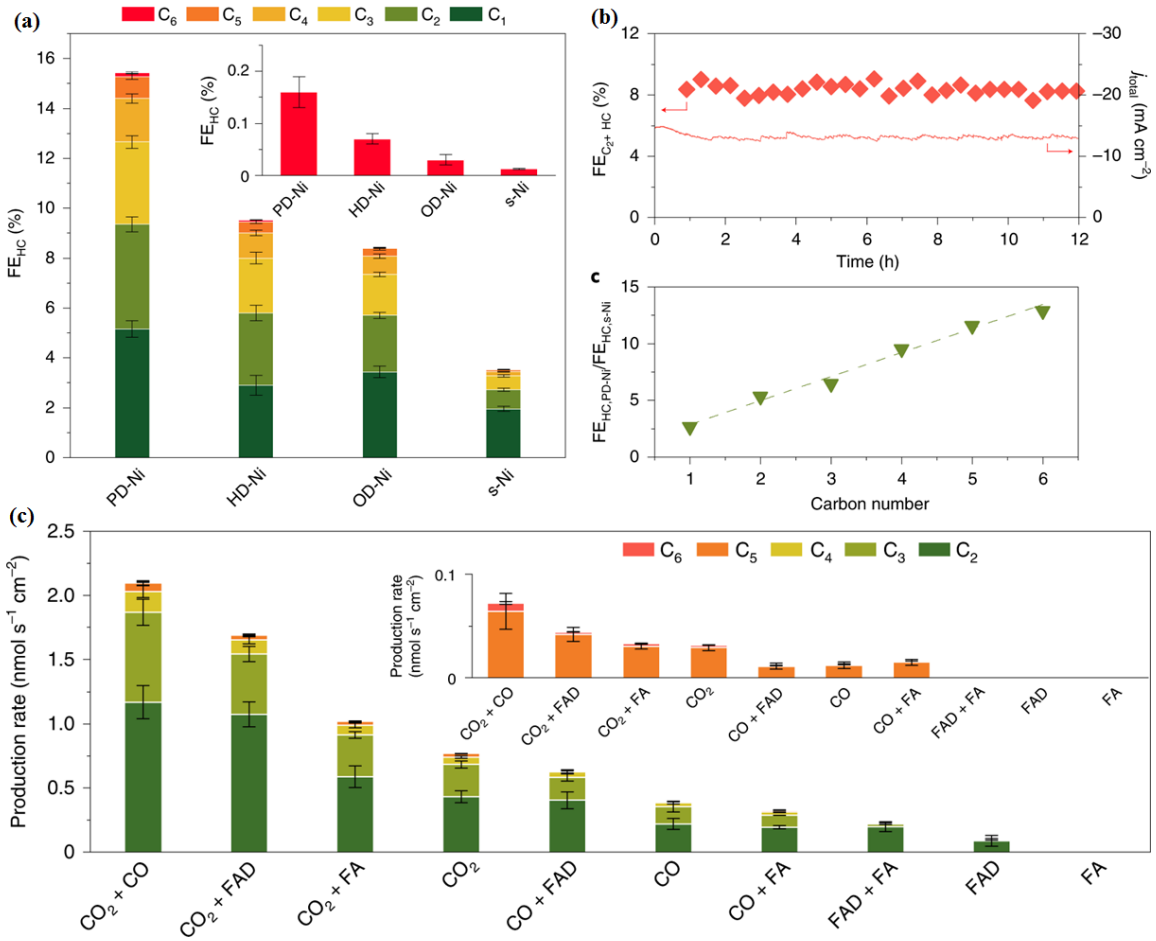

Figure 6. (a and b) CO_2 electroreduction to hydrocarbons on Ni catalysts. (c) Experimental screening of key intermediates in the CO_2RR on PD-Ni [62] Copyright Nature 2022.

intermediates, allowing for continuous CO_2 reduction without catalyst deactivation [62]. The identification of a family of earth-abundant catalysts capable of producing long-chain hydrocarbons through a mechanism distinct from copper-based catalysts could significantly advance global efforts to establish a net-zero carbon cycle for the production of synthetic fuels [23, 56, 62, 68–71].

The search for substitute catalysts that can raise CO_2RR efficiency and selectivity toward long-chain hydrocarbons has garnered more attention recently. Because of its exceptional capacity to adsorb and activate CO_2 and CO intermediates under specific circumstances, nickel (Ni) has become a viable contender. Ni catalysts' catalytic capabilities are further improved by the addition of surface polarization, especially when it comes to promoting the C-C coupling events required for the synthesis of long-chain hydrocarbons. The capacity of polarized Ni catalysts to create long-chain hydrocarbons with great selectivity and efficiency is the main topic of a study that examines their function in CO_2 electroreduction [62]. The results shed light on the mechanisms governing C-C interaction on Ni surfaces and demonstrate the potential of polarized Ni catalysts as a competitive substitute for conventional Cu-based systems in the generation of sustainable hydrocarbons.

Improved C-C coupling efficiency and enhanced CO adsorption significantly impact the catalytic performance of polarized nickel (Ni) surfaces in CO_2 electroreduction, which is crucial for the synthesis of long-chain hydrocarbons. The effect of Ni polarization on the adsorption and insertion processes during CO_2 reduction is illustrated in figure 7 (a-c). When Ni is polarized, the electric field at the surface strengthens the interaction between Ni atoms and CO molecules, leading to a higher surface coverage of CO. This enhanced CO adsorption is critical, as it facilitates the incorporation of CO into reactive intermediates, the first step in C-C bond formation. The increased reactivity of these intermediates on the polarized Ni surface further promotes carbon chain formation, which is essential for synthesizing long-chain hydrocarbons.

A comparative analysis of these two catalysts is presented in figure 7 (d&e), which delves deeper into the initial C-C coupling processes during CO_2 reduction on polarized Ni and Cu surfaces. The strong CO adsorption on the polarized Ni surface leads to a higher local concentration of CO molecules, increasing the likelihood of C-C bond formation. This C-C coupling is more efficient on polarized Ni, as the surface polarization stabilizes the resulting C_2 intermediates and strengthens their adsorption, thus improving the overall thermodynamics of the process. In contrast, the Cu surface weakens CO adsorption, resulting in lower CO coverage and a reduced chance of efficient C-C coupling. As a result, the synthesis of long-chain hydrocarbons on Cu is less effective than on Ni. Overall, these findings highlight the critical role of surface polarization on Ni catalysts in enhancing the efficiency of CO_2 electroreduction, particularly for promoting long-chain hydrocarbon synthesis. Polarized Ni surfaces outperform Cu due to their stronger CO adsorption and improved C-C interaction, providing valuable insights for the development of more efficient catalysts for sustainable fuel production [62].

The polarization of Ni-based catalysts significantly influences product selectivity in CO_2 reduction by modulating the adsorption strength of key intermediates. Increased polarization enhances CO adsorption on the Ni surface, facilitating C-C coupling and promoting the formation of multi-carbon hydrocarbons. This effect reduces the competition with the hydrogen evolution reaction (HER) and stabilizes reaction intermediates, leading to higher selectivity for long-chain products. Additionally, polarization can alter the electronic structure of Ni, improving its catalytic efficiency for CO_2 conversion and minimizing catalyst deactivation. Let me know if you need further refinements or a more detailed explanation in your document.

Mechanism of CO_2 reduction

The first step of the mechanism is CO_2 gas adsorption on the surface of the metal (silver (111) in the case of figure 8 (a)), followed by the addition of a proton, resulting in formate formation [72]. In the next step, CO is formed from formate, which is desorbed in the later step. CO gas is then adsorbed on a metal surface (Cu (100) presented in figure 8 (b)), followed by the addition of a proton and formation of metal carbide. Later, the addition of one proton in each step finally results in the formation of methane gas. However, CO gas adsorption on the copper surface can follow another mechanism, resulting in the formation of ethylene gas. CO gas adsorption can result in dimerization, followed by the addition of two protons, followed by the removal of the hydroxyl group. The next steps include the addition of a proton, followed by the removal of another oxygen. Then, protons are again added step by step, resulting in the formation of ethylene gas. However, it is important to mention here that application of different amounts of potentials can alter the reaction free energy for different mechanistic steps. The rate-determining steps (RDS) for the formation of different products are highlighted in a grey color. The presence of cations can play an important role in the reaction mechanism. The presence of potassium ions changes the coordination number and bader charge as presented in figure 8 (d). Cations stabilize the intermediates as well as facilitate the electron transfer from metal electrodes to reaction intermediates. Through the partial density of states analyses (PDOS), figure 8 (f) shows that the interaction of cations with the reaction intermediates results in a downward shift of the lowest unoccupied molecular orbital (LUMO), thus facilitating electrochemical conversion of CO_2.

Quantitative comparison of catalyst performance in CO_2RR

The performance of CO_2 reduction catalysts varies significantly depending on their composition, structure, and reaction conditions. Copper-based catalysts are widely studied for their ability to produce multi-carbon (C_{2+}) products, with recent studies reporting Faradaic efficiencies (FE) of $\sim 60-70\%$ for ethylene (C_2H_4) and ethanol (C_2H_5OH) at current densities exceeding 300 mA/cm^2. However, selectivity remains a challenge due to competing hydrogen evolution reaction (HER). In contrast, nickel-based cata-

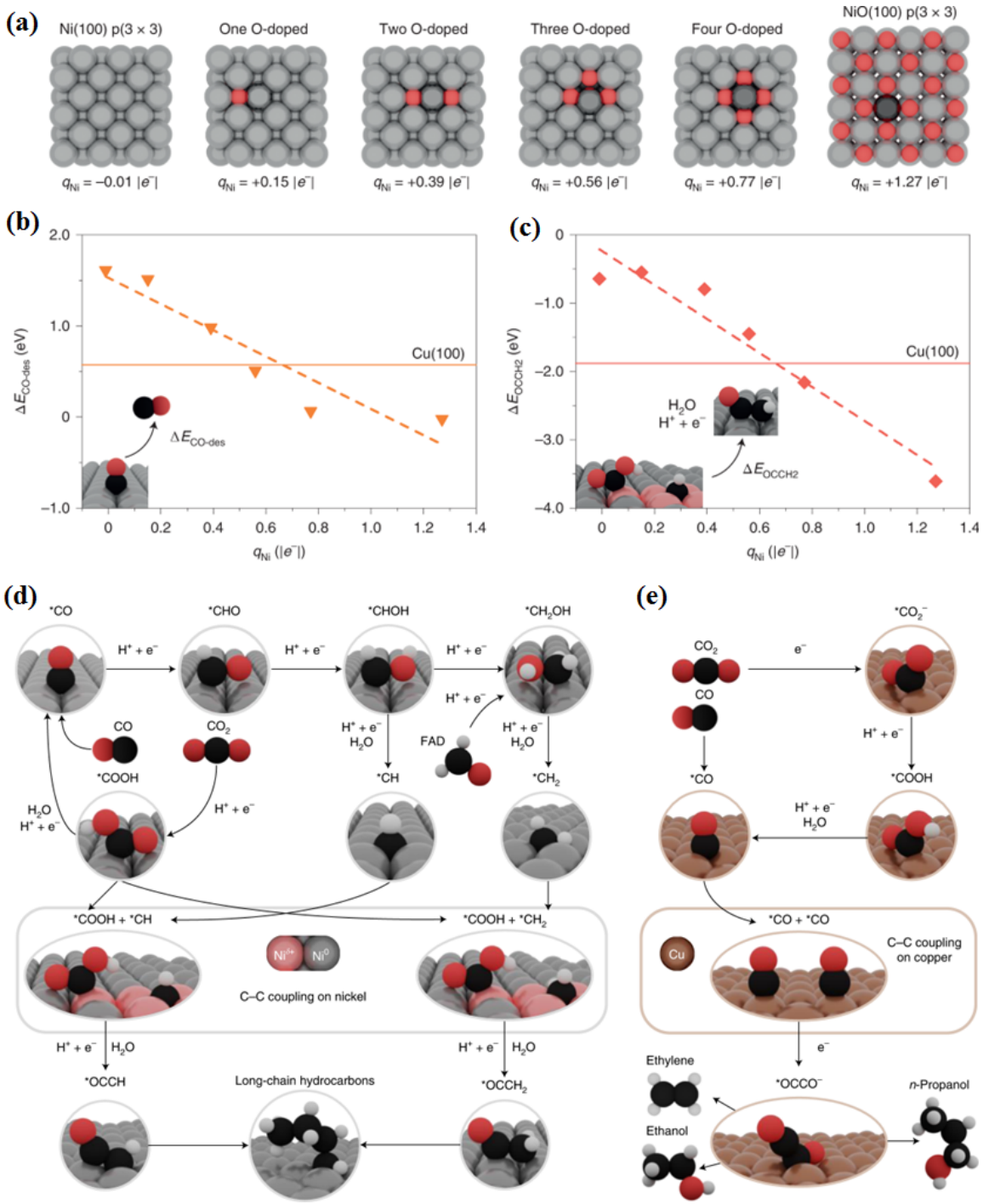

Figure 7. (a to c) Effect of Ni polarization on the adsorption and insertion steps during CO_2 reduction. (d) Initial C-C coupling steps in CO_2 reduction on polarized nickel and copper surfaces [62] Copyright Nature 2022.

lysts, particularly polarized Ni catalysts, have demonstrated enhanced C-C coupling capabilities, achieving FE values of $\sim 16\%$ for C_{3+} hydrocarbons and partial current densities of ~ 0.91 mA/cm^2, surpassing many Cu-based alternatives. Single-atom catalysts (SACs), such as Ni-N-C and Fe-N-C systems, exhibit superior turnover frequencies (TOF) of $0.2 - 0.5$ s^{-1} and high selectivity toward CO ($> 90\%$), making them ideal for CO production rather than hydrocarbon formation. Meanwhile, molecular catalysts, leveraging bimetallic and ligand-tuned active sites, have enabled improved CO_2 binding and reduction kinetics, achieving over 90% selectivity for formic acid (HCOOH) at overpotentials as low as 0.5 V.

Despite these advancements, challenges remain in achieving higher stability and long-term durability. For example, Cu-based catalysts suffer from deactivation due to surface reconstruction, whereas Ni-based catalysts demonstrate enhanced stability under high current densities. A comparison of performance for different catalysts has been given in Table 3. Future research should focus on optimizing reaction kinetics, active site engineering, and electrolyte effects to further improve catalyst efficiency and commercial viability.

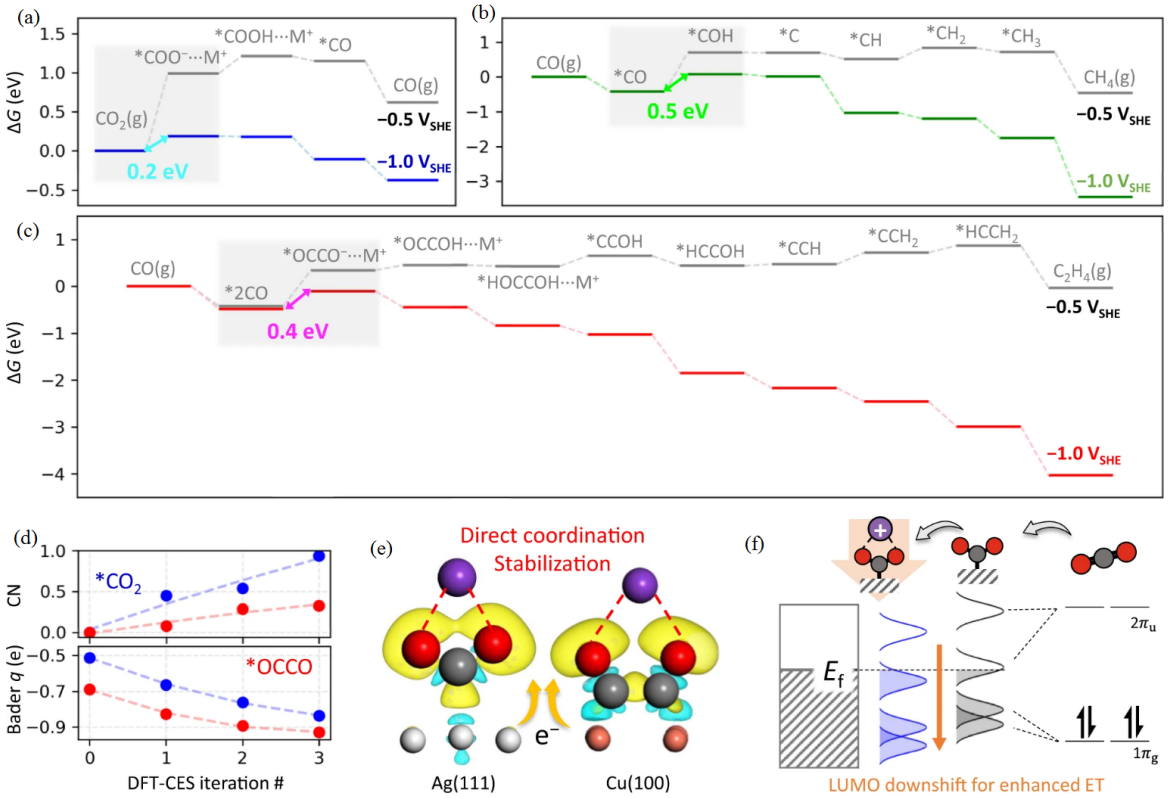

Figure 8. (a-c) Reaction free energy (ΔG) diagrams illustrating CO_2 reduction to CO on Ag (111) (a), CO conversion to CH_4 on Cu (100) (b), and CO transformation to C_2H_4 on Cu (100) (c). The applied potentials are −0.5 and −1 VSHE. The asterisk (*) represents adsorbed states, with energetically favorable pathways highlighted among various possibilities. Cation-coordinated intermediates are denoted by the addition of M+. The rate-determining step (RDS) is marked by a grey-shaded region. (d) Variation in the coordination number (CN) of K^+ with $*CO_2$ and *OCCO, along with the corresponding changes in Bader charge (Bader q) for these intermediates, as determined through DFT-CES iterations at −0.5 VSHE. (e) Cation interactions with intermediates not only enhance their stability but also facilitate electron transfer from the metal electrodes. Water molecules are excluded for clarity. (f) A schematic representation of CO_2 energy level modifications, derived from projected density of states (PDOS) analysis [72] Copyright Nature.

Limitations of molecular catalysts compared to metal-based catalysts

While molecular catalysts offer advantages such as tunable active sites, enhanced C-C coupling, and the ability to operate under mild conditions, they also have inherent limitations compared to conventional metal-based catalysts. One of the major challenges is their limited stability under electrochemical conditions, as many molecular catalysts undergo degradation, ligand dissociation, or structural reorganization over extended operation. Additionally, their turnover frequencies (TOF), typically in the range of $0.01 - 0.5\ s^{-1}$, are often lower than those of metal-based catalysts, which can exceed $1\ s^{-1}$ in optimized systems. Another drawback is their relatively low current densities, which can restrict large-scale implementation. In contrast, metal-based catalysts, such as Cu and Ni-based systems, exhibit higher Faradaic efficiencies (> 60% for C_2 products) and greater tolerance to industrial operating conditions. Furthermore, molecular catalysts often require precise ligand design and synthesis, increasing their cost and complexity in comparison to scalable metallic electrodes. Overcoming these limitations requires advancements in ligand stabil-

Table 3. Summary table comparing different catalyst types in CO_2 reduction, focusing on activity, stability, and selectivity.

Catalyst Type	Faradaic Efficiency (FE)	Turnover Frequency (TOF)	Current Density	Stability	Selectivity
Copper-based	∼ 60 − 70% (C_2 products)	$0.1-1\ s^{-1}$	>300 mA/cm^2	Moderate (Surface reconstruction)	Ethylene (C_2H_4), Ethanol (C_2H_5OH)
Nickel-based	∼16% (C_{3+} hydrocarbons)	$0.05-0.5\ s^{-1}$	∼0.91 mA/cm^2	High (Stable under high current)	C_3-C_6 hydrocarbons
Single-Atom (SACs)	>90% (CO)	$0.2-0.5\ s^{-1}$	10−50 mA/cm^2	High (Strong metal-support interactions)	CO production
Molecular Catalysts	>90% (HCOOH)	$0.01-0.5\ s^{-1}$	Low (∼10 mA/cm^2)	Low (Ligand degradation)	Formic acid (HCOOH)
Bimetallic Catalysts	∼50−80% (C_{2+} products)	$0.3-1.2\ s^{-1}$	100−250 mA/cm^2	Moderate (Alloy stability issues)	Ethanol, Propanol

ity, catalyst immobilization, and hybrid molecular-metal systems, which could combine the selectivity of molecular catalysts with the durability of metal-based catalysts for improved CO_2 conversion performance.

2. Conclusion, prospects, and future recommendations

One of the most important technologies in the global endeavor to reduce carbon emissions and reach carbon neutrality is the electrochemical CO_2 reduction reaction (CO_2RR). The discovery of molecular catalysts and electrochemical Fischer-Tropsch (FT) processes, in particular, has led to improvements in selectivity and efficiency in the conversion of CO_2 into valuable hydrocarbons. This article focuses on the advancements made in CO_2 electroreduction to produce C_1, C_2, and higher hydrocarbons, highlighting the possibility that these processes could eventually supplant conventional methods that rely on fossil fuels. The commercial feasibility of CO_2RR technologies depends on the development of strong, long-lasting catalysts that can continue to operate at high-performance levels in industrial settings. Notwithstanding, notable hindrances such as catalyst stability, energy efficiency, and product selectivity continue to exist. To fully utilize CO_2 electroreduction's potential for closing the carbon cycle and promoting sustainability, these problems must be resolved.

Future Recommendations:

1. *Catalyst Design and Stability*: The discovery of more stable catalysts that perform well in both acidic and alkaline conditions should be the main goal of future research. Investigating new materials could boost C-C coupling and improve selectivity for higher hydrocarbons. One example of such a material is a molecular catalyst with two active sites.
2. *Scalability and Industrial Integration*: Resolving the scalability issue with CO_2 electroreduction methods is crucial to achieving success outside of the laboratory. The creation of integrated systems that integrate the processes of CO_2 capture, storage, and conversion with the use of renewable energy sources is essential to guaranteeing the commercial viability of these technologies.
3. *Process Optimization*: To increase efficiency and selectivity, ongoing efforts should be made to adjust the reaction parameters, including temperature, pressure, and electrolyte composition. Examining how external elements like surface polarization and the application of electric fields function could improve CO_2RR system performance even more.
4. *Minimizing Side Reactions*: The competitive hydrogen evolution process (HER) is a major obstacle in CO_2 electroreduction. Subsequent research ought to delve into methods of inhibiting HER, including altering the surface or creating specific catalysts that give precedence to the reduction of CO_2 instead of the creation of hydrogen.
5. *Long-Term Performance and Durability*: Commercial deployment of CO_2 electroreduction catalysts depends on their long-term stability. Understanding catalyst degradation mechanisms and creating strategies to extend catalysts' active lives should be the main goals of the research.
6. *Collaborative Research and Policy Support*: Regulators, industry, and academics must work together to expedite the development and implementation of CO_2RR technologies. Investments in research and development as well as policy frameworks that encourage carbon capture and utilization will be essential for the advancement of this profession.

Authors contributions
Authors have contributed equally in preparing and writing the manuscript.

Availability of data and materials
The data that support the findings of this study are available from the corresponding author, upon reasonable request.

Conflict of interests
The author declare that they have no known competing financial interests or personal relationships that could have appeared to influence the work reported in this paper.

References

[1] B. Belsa, L. Xia, V. Golovanova, B. Polesso, A. Pinilla-Sánchez, L. San Martín, J. Ye, C.-T. Dinh, and F.P. García de Arquer. *Nat. Rev. Mater.*, **9**(2024):535–549, .
DOI: https://doi.org/10.1038/s41578-024-00696-9.

[2] B. Pickering, F. Lombardi, and S. Pfenninger. *Joule*, **6**(2022):1253–1276.
DOI: https://doi.org/10.1016/j.joule.2022.05.009.

[3] E. R. Nesbitt. *Ind. Biotechnol.*, **16**(2020):147–163.
DOI: https://doi.org/10.1089/ind.2020.29217.ern.

[4] C. Hepburn, E. Adlen, J. Beddington, E. A. Carter, S. Fuss, N. Mac Dowell, J. C. Minx, P. Smith, and C. K. Williams. *Nature*, **575**(2019):87–97.
DOI: https://doi.org/10.1038/s41586-019-1681-6.

[5] M. H. Barecka, J. W. Ager, and A. A. Lapkin. *iScience*, **24**(2021).
DOI: https://doi.org/10.1016/j.isci.2021.102514.

[6] P. Markewitz, W. Kuckshinrichs, W. Leitner, J. Linssen, P. Zapp, R. Bongartz, A. Schreiber, and T. E. Müller. *Energy Environ. Sci.*, **5**(2012):7281–7305.
DOI: https://doi.org/10.1039/C2EE03403D.

[7] S. Kaiser, S. Gold, and S. Bringezu. *Resour. Conserv. Recycl.*, **184**(2022):106422.
DOI: https://doi.org/10.1016/j.resconrec.2022.106422.

[8] E. C. Ra, K. Y. Kim, E. H. Kim, H. Lee, K. An, and J. S. Lee. *ACS Catal.*, **10**(2020):11318–11345.
DOI: https://doi.org/10.1021/acscatal.0c02930.

[9] W. Fang, W. Guo, R. Lu, Y. Yan, X. Liu, D. Wu, F. M. Li, Y. Zhou, C. He, and C. Xia. *Nature*, **626**(2024):86–91.
DOI: https://doi.org/10.1038/s41586-023-06917-5.

[10] Y. Zhao, J. Zhang, X. Guo, X. Cao, S. Wang, H. Liu, and G. Wang. *Chem. Soc. Rev.*, **52**(2023):3215–3264, .
DOI: https://doi.org/10.1039/D2CS00698G.

[11] J. Qu, X. Cao, L. Gao, J. Li, L. Li, Y. Xie, Y. Zhao, J. Zhang, M. Wu, and H. Liu. *Nano-Micro Lett.*, **15**(2023):178.
DOI: https://doi.org/10.1007/s40820-023-01146-x.

[12] M. Asif, C. Yao, Z. Zuo, M. Bilal, H. Zeb, S. Lee, Z. Wang, and T. Kim. *J. Ind. Eng. Chem.*, (2024), .
DOI: https://doi.org/10.1016/j.jiec.2024.09.035.

[13] S. Ahmed, S. S. Bibi, M. Irshad, M. Asif, M. K. Khan, and J. Kim. *Top. Catal.*, **67**(2024):363–376.
DOI: https://doi.org/10.1007/s11244-023-01888-3.

[14] M. Asif, S. S. Bibi, S. Ahmed, M. Irshad, M. S. Hussain, H. Zeb, M. K. Khan, and J. Kim. *Chem. Eng. J.*, (2023):145381, .
DOI: https://doi.org/10.1016/j.cej.2023.145381.

[15] J. Chen, L. Xu, and B. Shen. *Renew. Sustainable Energy Rev.*, **199**(2024):114516.
DOI: https://doi.org/10.1016/j.rser.2024.114516.

[16] N. Zhu, X. Zhang, N. Chen, J. Zhu, X. Zheng, Z. Chen, T. Sheng, Z. Wu, and Y. Xiong. *J. Am. Chem. Soc.*, **145**(2023):24852–24861, .
DOI: https://doi.org/10.1021/jacs.3c09307.

[17] J. Zhang, Y. Wang, Z. Li, S. Xia, R. Cai, L. Ma, T. Zhang, J. Ackley, S. Yang, and Y. Wu. *Adv. Sci.*, **9**(2022):2200454, .
DOI: https://doi.org/10.1002/advs.202200454.

[18] Y. Li, X. F. Lu, S. Xi, D. Luan, X. Wang, and X. W. Lou. *Angew. Chem. Int. Ed.*, **61**(2022):e202201491, .
DOI: https://doi.org/10.1002/anie.202201491.

[19] J. Gu, S. Liu, W. Ni, W. Ren, S. Haussener, and X. Hu. *Nat. Catal.*, **5**(2022):268–276.
DOI: https://doi.org/10.1038/s41929-022-00761-y.

[20] Y. F. Lu, L. Z. Dong, J. Liu, R. X. Yang, J. J. Liu, Y. Zhang, L. Zhang, Y. R. Wang, S. L. Li, and Y. Q. Lan. *Angew. Chem.*, **133**(2021):26414–26421.
DOI: https://doi.org/10.1002/ange.202111265.

[21] Y. C. Tan, K. B. Lee, H. Song, and J. Oh. *Joule*, **4**(2020):1104–1120.
DOI: https://doi.org/10.1016/j.joule.2020.03.013.

[22] D.-H. Nam, O. S. Bushuyev, J. Li, P. De Luna, A. Seifitokaldani, C.-T. Dinh, F. P. García de Arquer, Y. Wang, Z. Liang, and A. H. Proppe. *J. Am. Chem. Soc.*, **140**(2018):11378–11386.
DOI: https://doi.org/10.1021/jacs.8b06407.

[23] J. Qiao, Y. Liu, F. Hong, and J. Zhang. *Chem. Soc. Rev.*, **43**(2014):631–675.
DOI: https://doi.org/10.1039/c3cs60323g.

[24] Y. Hori, A. Murata, R. Takahashi, and S. Suzuki. *J. Am. Chem. Soc.*, **109**(1987):5022–5023, .
DOI: https://doi.org/10.1021/ja00250a044.

[25] A. Ehsani, M. Hadi, E. Kowsari, S. Doostikhah, and J. Torabian. *Iran. J. Catal.*, **7**(2017). URL https://oiccpress.com/ijc/article/view/3967.

[26] E. Zarei, M. R. Jamali, and J. Bagheri. *Iran. J. Catal.*, **8**(2018):165–177. URL https://journals.iau.ir/article-607339.html.

[27] A. Rostami-Vartooni, A. N. Golikand, and M. Bagherzadeh. *Iran. J. Catal.*, **7**(2017). URL https://oiccpress.com/ijc/article/view/3983.

[28] C. Zhu, A. Chen, J. Mao, G. Wu, S. Li, X. Dong, G. Li, Z. Jiang, Y. Song, and W. Chen. *Small Struct.*, **4**(2023):2200328, .
DOI: https://doi.org/10.1002/sstr.202200328.

[29] Y. Liu, H. Liu, C. Wang, Y. Wang, J. Lu, and H. Wang. *Electrochem. Commun.*, **150**(2023):107474, .
DOI: https://doi.org/10.1016/j.elecom.2023.107474.

[30] Z. Zhou, S. Liang, J. Xiao, T. Zhang, M. Li, W. Xie, and Q. Wang. *J. Energy Chem.*, **84**(2023):277–285, .
DOI: https://doi.org/10.1016/j.jechem.2023.04.040.

[31] W. Guo, X. Tan, S. Jia, S. Liu, X. Song, X. Ma, L. Wu, L. Zheng, X. Sun, and B. Han. *CCS Chem.*, **6**(2024):1231–1239.
DOI: https://doi.org/10.31635/ccschem.023.202303138.

[32] Q. Wu, R. Du, P. Wang, G. I. Waterhouse, J. Li, Y. Qiu, K. Yan, Y. Zhao, W.-W. Zhao, and H.-J. Tsai. *ACS Nano*, **17**(2023):12884–12894.
DOI: https://doi.org/10.1039/D4TA00502C.

[33] M. Ye, T. Shao, J. Liu, C. Li, B. Song, and S. Liu. *Appl. Surf. Sci.*, **622**(2023):156981.
DOI: https://doi.org/10.1016/j.apsusc.2023.156981.

[34] B. Belsa, L. Xia, V. Golovanova, B. Polesso, A. Pinilla-Sánchez, L. San Martín, J. Ye, C.-T. Dinh, and F.P. García de Arquer. *Nat. Rev. Mater.*, **9**(2024):535–549, .
DOI: https://doi.org/10.1038/s41578-024-00696-9.

[35] Y. R. Du, X. Q. Li, X. X. Yang, G. Y. Duan, Y. M. Chen, and B. H. Xu. *Small*, **20**(2024):2402534.
DOI: https://doi.org/10.1002/smll.202402534.

[36] C. Yang, R. Wang, C. Yu, J. Xiao, Z. Huang, B. Lv, H. Zhao, X. Wu, and G. Jing. *Chem. Eng. J.*, **484**(2024):149710.
DOI: https://doi.org/10.1016/j.cej.2024.149710.

[37] T. Deng, S. Jia, S. Han, J. Zhai, J. Jiao, X. Chen, C. Xue, X. Xing, W. Xia, and H. Wu. *Front. Energy*, **18**(2024):80–88.
DOI: https://doi.org/10.1007/s11708-023-0898-0.

[38] L.-X. Liu, Y. Cai, H. Du, X. Lu, X. Li, F. Liu, J. Fu, and J.-J. Zhu. *ACS Appl. Mater. Interfaces*, **15**(2023):16673–16679, .
DOI: https://doi.org/10.1021/acsami.2c21902.

[39] Z.-Y. Zhang, H. Tian, L. Bian, S.-Z. Liu, Y. Liu, and Z.-L. Wang. *J. Energy Chem.*, **83**(2023):90–97, .
DOI: https://doi.org/10.1016/j.jechem.2023.04.034.

[40] X. Meng, H. Huang, X. Zhang, L. Hu, H. Tang, M. Han, F. Zheng, and H. Wang. *Adv. Funct. Mater.*, **34**(2024):2312719.
DOI: https://doi.org/10.1002/adfm.202312719.

[41] R. Zhang, J. Zhang, S. Wang, Z. Tan, Y. Yang, Y. Song, M. Li, Y. Zhao, H. Wang, and B. Han. *Angew. Chem. Int. Ed.*, **63**(2024):e202405733, .
DOI: https://doi.org/10.1002/anie.202405733.

[42] H. Wang, A. Gao, A. Bari, M. Gu, X. Zhang, and G. Wang. *ACS Appl. Nano Mater.*, **7**(2024):6810–6819, .
DOI: https://doi.org/10.1021/acsanm.3c04961.

[43] M. Wang, C. Chen, S. Jia, S. Han, X. Dong, D. Zhou, T. Yao, M. Fang, M. He, and W. Xia. *Chem. Sci.*, **15**(2024):8451–8458, .
DOI: https://doi.org/10.1039/D4SC01735H.

[44] T. Zhao, X. Zong, J. Liu, J. Chen, K. Xu, X. Wang, X. Chen, W. Yang, F. Liu, and M. Yu. *Appl. Catal. B: Environ.*, **340**(2024):123281, .
DOI: https://doi.org/10.1016/j.apcatb.2023.123281.

[45] X.-M. Hu, H.-Q. Liang, A. Rosas-Hernández, and K. Daasbjerg. *Chem. Soc. Rev.*, (2025), .
DOI: https://doi.org/10.1039/D4CS00480A.

[46] A. Dourani and M. Haghgoo. *Iran. J. Catal.*, **14**(2024):1–13.
DOI: https://doi.org/10.57647/j.ijc.2024.1403.30.

[47] S. Overa, B. H. Ko, Y. Zhao, and F. Jiao. *Acc. Chem. Res.*, **55**(2022):638–648.
DOI: https://doi.org/10.1021/acs.accounts.1c00674.

[48] R. Sharifian, R. Wagterveld, I. Digdaya, C.-X. Xiang, and D. Vermaas. *Energy Environ. Sci.*, **14**(2021):781–814.
DOI: https://doi.org/10.1039/D0EE03382K.

[49] H. Li, M. E. Zick, T. Trisukhon, M. Signorile, X. Liu, H. Eastmond, S. Sharma, T. L. Spreng, J. Taylor, and J. W. Gittins. *Nature*, (2024):1–6, .
DOI: https://doi.org/10.1038/s41586-024-07449-2.

[50] N. McQueen, P. Kelemen, G. Dipple, P. Renforth, and J. Wilcox. *Nat. Commun.*, **11**(2020):3299.
DOI: https://doi.org/10.1038/s41467-020-16510-3.

[51] Y. Hu, J. Gong, H. Zeb, H. Lan, M. Asif, H. Xia, and M. Du. *Chem. Commun.*, **60**(2024):10618–10628, .
DOI: https://doi.org/10.1039/D4CC03964E.

[52] M. Ahmadi Khoshooei, X. Wang, G. Vitale, F. Formalik, K. O. Kirlikovali, R. Q. Snurr, P. Pereira-Almao, and O. K. Farha. *Science*, (2024):540–546.
DOI: https://doi.org/10.1126/science.adl1260.

[53] M. S. Hussain, S. Ahmed, M. Irshad, S. S. Bibi, M. Asif, F. Sher, and M. K. Khan. *Nano Mater. Sci.*, (2024).
DOI: https://doi.org/10.1016/j.nanoms.2024.09.001.

[54] N. Sakamoto, K. Sekizawa, S. Shirai, T. Nonaka, T. Arai, S. Sato, and T. Morikawa. *Nat. Catal.*, (2024):1–11.
DOI: https://doi.org/10.1038/s41929-024-01147-y.

[55] Z. Weng, Y. Wu, M. Wang, J. Jiang, K. Yang, S. Huo, X.-F. Wang, Q. Ma, G. W. Brudvig, and V. S. Batista. *Nat. Commun.*, **9**(2018): 415.
DOI: https://doi.org/10.1038/s41467-018-02819-7.

[56] S. Ren, Z. Zhang, E. W. Lees, A. G. Fink, L. Melo, C. Hunt, D. J. Dvorak, W. Y. Wu, E. R. Grant, and C. P. Berlinguette. *Chem. Eur. J.*, **28**(2022):e202200340.
DOI: https://doi.org/10.1002/chem.202200340.

[57] H. Q. Liang, T. Beweries, R. Francke, and M. Beller. *Angew. Chem.*, **134**(2022):e202200723.
DOI: https://doi.org/10.1002/ange.202200723.

[58] M. Li, Y. Ma, J. Chen, R. Lawrence, W. Luo, M. Sacchi, W. Jiang, and J. Yang. *Angew. Chem. Int. Ed.*, **60**(2021):11487–11493, .
DOI: https://doi.org/10.1002/anie.202102606.

[59] F. Li, A. Thevenon, A. Rosas-Hernández, Z. Wang, Y. Li, C. M. Gabardo, A. Ozden, C. T. Dinh, J. Li, and Y. Wang. *Nature*, **577**(2020):509–513, .
DOI: https://doi.org/10.1038/s41586-019-1782-2.

[60] M. Balamurugan, H. Y. Jeong, V. S. K. Choutipalli, J. S. Hong, H. Seo, N. Saravanan, J. H. Jang, K. G. Lee, Y. H. Lee, and S. W. Im. *Small*, **16**(2020):2000955.
DOI: https://doi.org/10.1002/smll.202000955.

[61] J.-M. Savéant. *Chem. Rev.*, **108**(2008):2348–2378.
DOI: https://doi.org/10.1021/cr068079z.

[62] Y. Zhou, A. J. Martín, F. Dattila, S. Xi, N. López, J. Pérez-Ramírez, and B. S. Yeo. *Nat. Catal.*, **5**(2022):545–554, .
DOI: https://doi.org/10.1038/s41929-022-00803-5.

[63] Y. Hori, A. Murata, R. Takahashi, and S. Suzuki. *Chem. Lett.*, **16**(1987):1665–1668, .
DOI: https://doi.org/10.1246/cl.1987.1665.

[64] Y. Hori, K. Kikuchi, A. Murata, and S. Suzuki. *Chem. Lett.*, **15**(1986): 897–898, .
DOI: https://doi.org/10.1246/cl.1986.897.

[65] Y. Yamazaki, M. Miyaji, and O. Ishitani. *J. Am. Chem. Soc.*, **144**(2022):6640–6660.
DOI: https://doi.org/10.1021/jacs.2c02245.

[66] Z. Ni, H. Liang, Z. Yi, R. Guo, C. Liu, Y. Liu, H. Sun, and X. Liu. *Coord. Chem. Rev.*, **441**(2021):213983.
DOI: https://doi.org/10.1016/j.ccr.2021.213983.

[67] C.-T. Dinh, T. Burdyny, M. G. Kibria, A. Seifitokaldani, C. M. Gabardo, F. P. García de Arquer, A. Kiani, J. P. Edwards, P. De Luna, and O. S. Bushuyev. *Science*, **360**(2018):783–787.
DOI: https://doi.org/10.1126/science.aas9100.

[68] M. Li and J.-N. Zhang. *Sci. China Chem.*, **66**(2023):1288–1317.
DOI: https://doi.org/10.1007/s11426-023-1565-5.

[69] X. Cao, J. Huo, L. Li, J. Qu, Y. Zhao, W. Chen, C. Liu, H. Liu, and G. Wang. *Adv. Energy Mater.*, **12**(2022):2202119.
DOI: https://doi.org/10.1002/aenm.202202119.

[70] M. Li, H. Wang, W. Luo, P. C. Sherrell, J. Chen, and J. Yang. *Adv. Mater.*, **32**(2020):2001848, .
DOI: https://doi.org/10.1002/adma.202001848.

[71] Y. Zheng, A. Vasileff, X. Zhou, Y. Jiao, M. Jaroniec, and S.-Z. Qiao. *J. Am. Chem. Soc.*, **141**(2019):7646–7659.
DOI: https://doi.org/10.1021/jacs.9b02124.

[72] S.-J. Shin, H. Choi, S. Ringe, D. H. Won, H.-S. Oh, D. H. Kim, T. Lee, D.-H. Nam, H. Kim, and C. H. Choi. *Nat. Commun.*, **13**(2022):5482.
DOI: https://doi.org/10.1038/s41467-022-33199-8.